

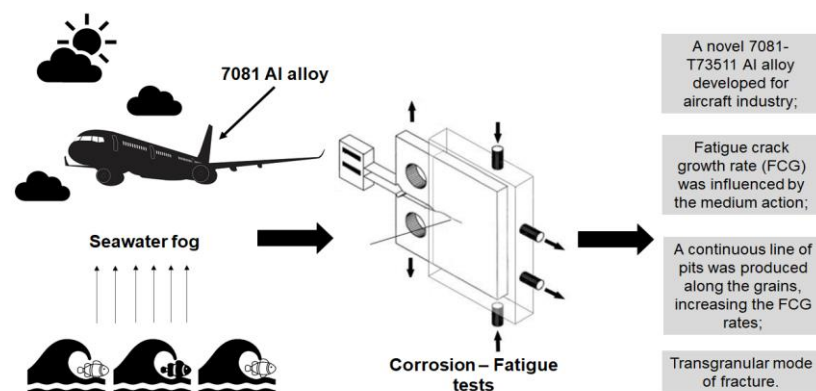
Short Communication | <http://dx.doi.org/10.17807/orbital.v14i4.17209>

Recent Studies of Corrosion - Fatigue Crack Growth on the 7081-T73511 Aluminium Alloy

Jéferson Aparecido Moreto  ^{a*} and Waldek Wladimir Bose Filho  ^b

This work aims to evaluate the effect of localized corrosion on the fatigue crack growth (FCG) resistance of the 7081-T73511 aluminium alloy. The understanding of this complex combined process was explained by the dissolution of adjacent 7081-T73511 aluminium matrix promoted by the $\text{Al}_7\text{Cu}_2\text{Fe}$ second-phase particle and the crack tip interaction time with the aggressive medium. Fracture surfaces produced in air and in sea water fog at the testing conditions applied here, basically present the same appearance, with a transgranular, cleavage-like cracking mode for $8 < DK < 30$ values.

Graphical abstract



Keywords

Aluminium alloy
Aircraft material
FCG tests
Fatigue
Corrosion tests

Article history

Received 20 Sept 2022
Accepted 05 Dec 2022
Available online 01 Jan 2023

Handling Editor: Adilson Beatriz

1. Introduction

It is well documented that 7xxx series aluminium alloys are widely used in several sectors owing to their low density, desirable strength as well as good corrosion resistance [1]. The corrosion resistance of aluminium in aqueous solutions is attributed to a passive layer of alumina (Al_2O_3) on its surface. However, when aluminium alloys are subjected to an aggressive environment, the passive film is broken, initiating a localised corrosion process [2, 3]. The 7081-T73511 aluminium alloy have already been studied by the present authors, namely in what concerns their global and localised corrosion processes and fatigue life (air, pre-corroded and salt-water fog conditions). As is already known, particles

containing Fe and Cu elements are cathodic with respect to the matrix, promoting dissolution of the aluminium matrix [4, 5]. Due to the above mentioned microgalvanic nature of the processes taking place, the influence of the corrosive media on the FCG curves is extremely required. In this sense, this survey may help to shed some light on the corrosion-fatigue mechanisms of the 7081-T73511 aluminium alloy. To the best of our knowledge, this is the first study concerning the influence of corrosive media on the fatigue properties of the 7081-T73511 aluminium alloy.

^a Institute of Exact Sciences, Naturals and Education, Federal University of Triângulo Mineiro (UFMT). Avenida Doutor Randolpho Borges Júnior, Univerdecidade, 38064200, Uberaba, MG, Brazil. ^b Department of Materials Engineering, São Carlos School of Engineering, University of São Paulo, Av. Trabalhador São-Carlense, 13566-590, São Carlos, SP, Brazil. *Corresponding author: jeferson.moreto.ufmt@gmail.com

2. Material and Methods

The 7081-T73511 Al alloy were used in the present work as received condition (extruded shapes). The nominal chemical composition (wt%) of the 7081-T73511 alloy is 7.24 Zn, 1.69 Cu, 0.02 Si, 0.04 Fe, 1.94 Mg and Al balance. The FCG rates were addressed considering T-L crack direction in the base material (BM) in air and 3.5 wt.% NaCl seawater fog environment. For this purpose, a 250 kN MTS servo-hydraulic machine was used, and to obtain the FCG (da/dN vs ΔK) curves, fatigue tests were carried out following the ASTM 647-15 [6]. The FCG tests were carried out under controlled load, sinusoidal waveform, 15 Hz (air) and 1 Hz (seawater fog environment) frequency, and $R = 0.1$. Here, all the tests were performed at room temperature 25 ± 2 °C. A special acrylic cell was designed for fatigue-corrosion tests and more details about the assembly may be obtained in reference [5].

Morphological analyzes were performed before and after the FCG tests.

3. Results and Discussion

Optical micrographs of microstructure of three orthogonal sections of 7081-T73511 Al alloy are presented in **Fig. 1 (a)**. **Figs. 1 (b-d)** exhibits the surface morphology of the alloy 7081 at different magnifications obtained by SEM. As shown in **Fig. 1 (a)**, the rolling process was very intense, and the SL and TL planes present recrystallized and elongated grains. **Fig. 1 (b)** displays an overview of Al matrix, including the distributions of dispersive submicrometric and continuous precipitates (see **Fig. 1 (c)**). Details concerning the Al_7Cu_2Fe particle can be seen in **Fig. 1 (d)**.

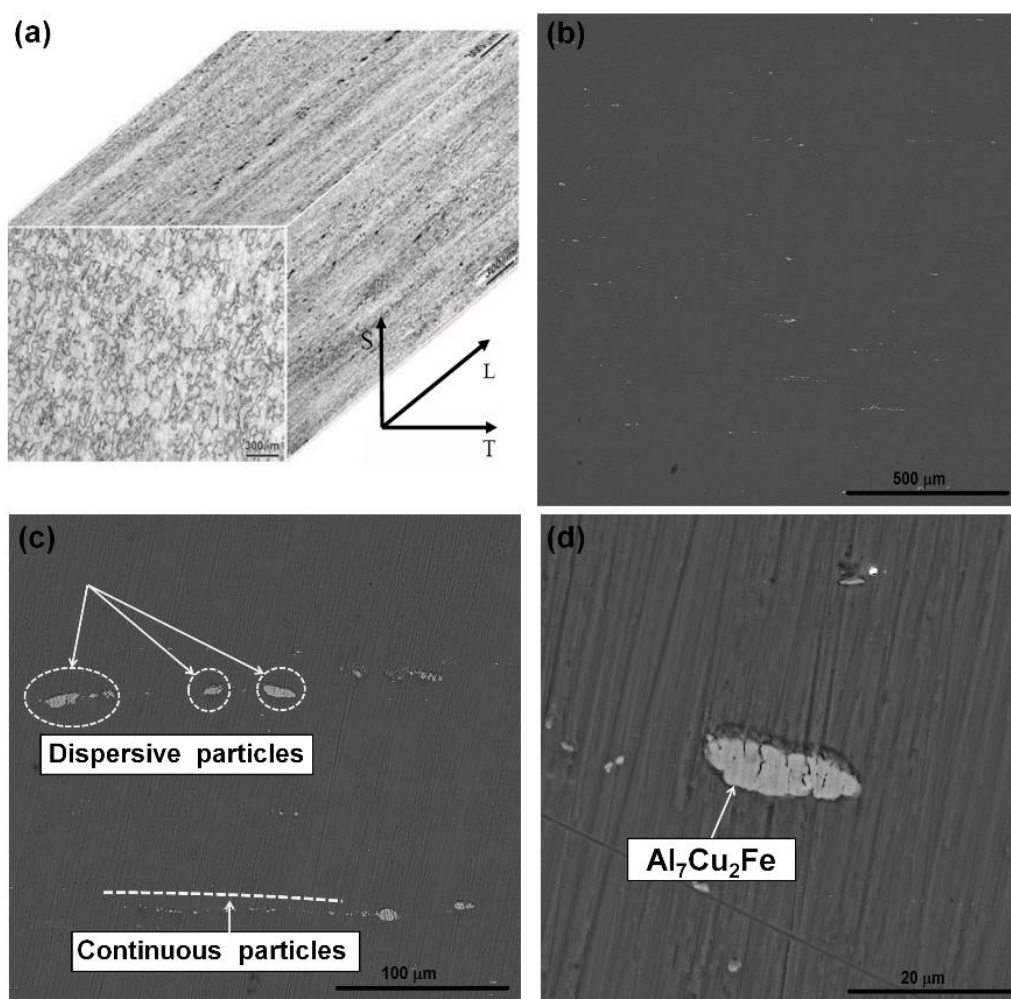


Figure 1. (a) Optical micrographs of microstructure of three orthogonal sections of 7081-T73511 Al alloy, (b) recrystallized and elongated grains on the SL and TL planes, (c) distribution of submicrometric dispersive and continuous particles and (d) details of the Al_7Cu_2Fe particle on the 7081-T73511 alloy surface. The Al_7Cu_2Fe particle composition was identified via energy-dispersive X-ray spectroscopy (EDX) and is not shown here.

From **Fig. 2** a linear correlation between the FCGR and ΔK (for $8 < \Delta K < 20$ MPa $m^{1/2}$) was observed. The Paris & Erdogan model, $\frac{da}{dN} = A\Delta K^m$, was used for further discussion. **A** and **m** account for material and environment effects (R , wave form and frequency are constant). The material constant m value was 3.41 and 2.83 for air and seawater fog environment, respectively, whilst **A** value was higher for the corrosive media

(2.31×10^{-7} versus 3.69×10^{-8}) [(mm/cycle)/ (MPa $m^{1/2}$)^m], respectively. As expected, the aggressive medium influenced the FCG rates of the 7081-T73511 alloy, demonstrating distinct behaviour at low and high ΔK values.

Fracture surfaces produced in air and in sea water fog at the testing conditions applied here, basically present the same appearance, with a transgranular, cleavage-like cracking

mode for $8 < \Delta K < 30$ values (see **Figure 2 (a)**). At lower ΔK values however (**Figure 2 (b)**), although the same cleavage-like appearance is still prevailing, subtle differences can be noticed in the distribution of flat, large, and smooth facets. At high ΔK values (**Figure 2 (c)**), at fatigue striations is more easily observable. Considering low values of ΔK , it was noticed a different behaviour for the alloy tested in air and seawater fog media. This finding is closely related to the crack tip interaction time with the aggressive medium. At low ΔK values ($\leq 15 \text{ MPa m}^{1/2}$), the passive thin film (Al_2O_3) that is spontaneously formed at the crack tip is broken by the stresses being applied, exposing the aluminium matrix to Cl^- ions.

As already demonstrated by these authors, the localised features of 7081-T73511 Al alloy are associated to the existence of second-phase particles that may be cathodic ($\text{Al}_7\text{Cu}_2\text{Fe}$) or anodic $\eta(\text{MgZn}_2)$ in relation to the aluminium matrix [7]. The presence of cathodic $\text{Al}_7\text{Cu}_2\text{Fe}$ particles promoted galvanic coupling, leading to the preferential dissolution of the nearby matrix, with formation of preferential sites for pitting initiation. Corrosion pits are initiated at the oxide layer in sites weakened by chloride attack, normally chemical or physical heterogeneities at the surface, such as inclusions, second-phase particles, flaws, mechanical damage, or dislocations [8]. As the cathodic IM particles are distributed along the grain length, a continuous line of pits is produced along these grains, increasing the FCG rates. **Fig. 3**

shows a schematic drawing of the proposed corrosion-fatigue mechanism for the 7081-T73511 aluminium alloy. The geometry of C(T) specimen used in the FCG tests is shown in **Fig. 3 (a)**. A schematic drawing of the proposed corrosion mechanism at the crack tip for the 7081-T73511 aluminium alloy is displayed in **Fig. 3 (b)**. The mechanism of pitting corrosion in 7081-T73511 aluminium alloy related to the galvanic coupling between the $\text{Al}_7\text{Cu}_2\text{Fe}$ second-phase particle and aluminium matrix is shown in **Fig. 3 (c)**. A general overview of 7081-T73511 aluminium surface, showing details of pits, grain boundaries as well as the crack path is presented in **Fig. 3 (d)**.

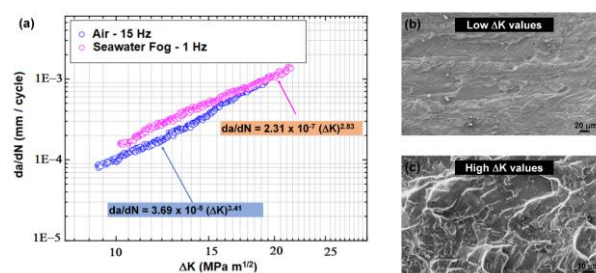


Fig. 2. (a) FCG curves of 7081-T73511 aluminium alloy in air and 0.6 mol L^{-1} seawater fog conditions (region II). The linear regression from the data extracted exclusively from Paris regime (region II) is not shown here. (b, c) the micrographs of only the sample tested in an aggressive medium for low and high ΔK values.

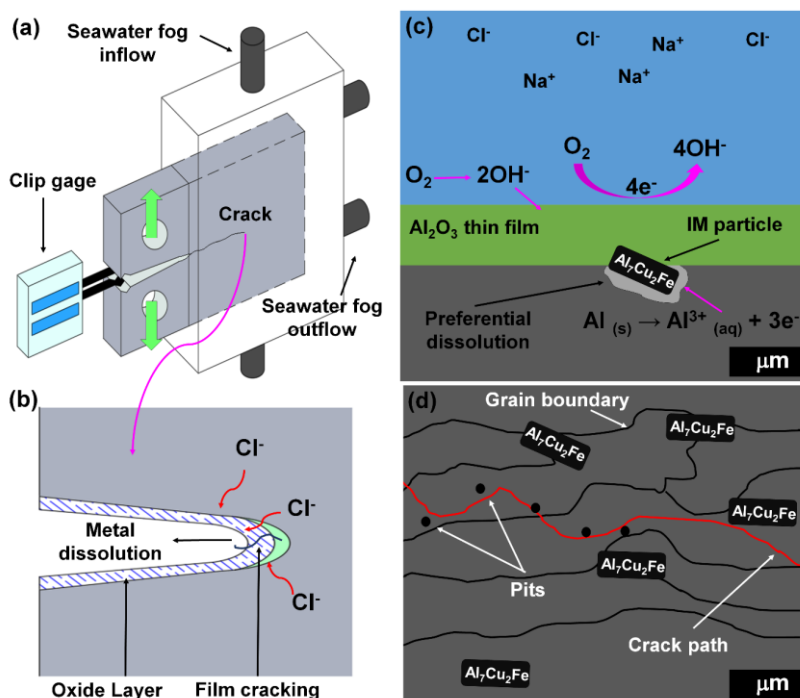


Fig. 3. (a) The geometry of C(T) specimen used in the FCG tests, (b-d) a schematic drawing of the proposed corrosion mechanism for the 7081-T73511 aluminium alloy, considering the $\text{Al}_7\text{Cu}_2\text{Fe}$ second-phase particle.

Finally, as ΔK increases the crack growth rate increases due to the mechanical loading, the medium effect is reduced due to less time for its interaction with the crack tip, and the dissolution micromechanisms at the crack tip becomes irrelevant. The micrographic analyses corroborate the fatigue crack growth curves, showing that the process is supported by the action of the medium.

4. Conclusions

This work may help to shed some light on the corrosion-fatigue synergism of the 7081-T73511 aluminium alloy. In this study, we concluded that the corrosive medium has affected the FCG rate of the 7081-T73511 aluminium alloy, which may

be explained by the dissolution of adjacent 7081-T73511 aluminium matrix promoted by the Al₇Cu₂Fe second-phase particles as well as the crack tip interaction time with the aggressive medium. The morphological analyses associated to the FCG curves displayed that the process is supported by the action of the medium. Additional studies should be performed in L-T and S-T orientations, since the microstructure plays an important role in the localised corrosion mechanisms of the 7xxx series aluminium alloy.

Acknowledgments

J. A. Moreto would like to acknowledge financial support received from the National Council of Technological and Scientific Development (CNPq-Brazil) (Grants 303659/2019-0 and 402988/2021-3), as well as Research Supporting Foundation of Minas Gerais State (FAPEMIG-Brazil) (Grant APQ-02276-18).

Author Contributions

Jeferson Aparecido Moreto: Conceptualization, Methodology, Validation, Formal analysis & Investigation. Waldek Wladimir Bose Filho: Formal Analysis.

References and Notes

- [1] Jiang, K.; Chen, L.; Zhang, Y.; Deng, Y. *Transactions of Nonferrous Metals Society of China* **2014**, *24*, 2117. [\[Crossref\]](#)

- [2] Shi, H.; Han, E.-H.; Liu, F.; Wei, T.; Zhu, Z.; Xu, D. *Corros. Sci.* **2015**, *98*, 150. [\[Crossref\]](#)
- [3] Ferreira, M. O. A.; Gelamo, R. V.; Marino, C. E. B.; da Silva, B. P.; Aoki, I. V.; da Luz, M. S.; Alexopoulos, N. D.; Leite, N.B.; Moreto, J. A. *Materialia* **2022**, *22*, 101407. [\[Crossref\]](#)
- [4] Moreto, J. A.; Marino, C. E. B.; Bose Filho, W. W.; Rocha, L. A.; Fernandes, J. C. S. *Corros. Sci.* **2014**, *84*, 30. [\[Crossref\]](#)
- [5] Gamboni, O. C.; Moreto, J. A.; Bonazzi, L. H. C.; Ruchert, C. O. F. T.; Bose Filho, W. W. *Mater. Res.* **2013**, *17*, 250. [\[Crossref\]](#)
- [6] ASTM - American Society for Testing and Materials, ASTM Standard E647-00, ASTM International, West Conshohocken, PA, 2017. [\[Crossref\]](#)
- [7] Fernandes, J. C. S.; Moreto, J. A.; Taryba, M.; Eugénio, S.; Sviallana, V. L.; Rocha, L. A.; Bose Filho, W. W. Trabalho completo do 10th International Symposium on Electrochemical Methods in Corrosion Research Maragogi, Brasil, 2012.
- [8] Metikoš-Huković, M.; Babić, R.; Grubač, Z.; Brinć, S. *Appl. Electrochem.* **1994**, *24*, 772. [\[Crossref\]](#)

How to cite this article

Moreto, J. A.; Bose Filho, W. W. *Orbital: Electron. J. Chem.* **2022**, *14*, 285. DOI: <http://dx.doi.org/10.17807/orbital.v14i4.17209>